Dynamics of s =1/2 disclinations in twisted nematics

J.A. Geurst, A.M.J. Spruijt, C.J. Gerritsma

Classification
Physics Abstracts
7.130

DYNAMICS OF $S = \frac{1}{2}$ DISCLINATIONS IN TWISTED NEMATICS

J. A. GEURST, A. M. J. SPRUIJT et C. J. GERRITSMA

Laboratoires de Recherche Philips, Eindhoven, Pays-Bas

(*Reçu le 19 septembre 1974, accepté le 27 février 1975*)

Résumé. — Les auteurs étudient du point de vue théorique et expérimental les lignes de disinclinaisons qui séparent des régions d'orientation opposée dans la structure twistée d'un cristal liquide nématique. Ils consacrent une attention particulière aux mouvements des lignes de disinclinaison induits par un champ magnétique. La comparaison des résultats théoriques et expérimentaux aboutit à une estimation des dimensions du cœur de la disinclinaison. On obtient accessoirement l'énergie élastique d'une ligne de disinclinaison. Ils donnent un modèle physique simple de l'effet combiné des forces magnétiques, induites par courbure et dissipatives qui agissent sur une ligne de disinclinaison.

Abstract. — Disclination lines separating regions with opposite twist in a twisted structure of a nematic liquid crystal are studied theoretically and experimentally. A particular study is made of magnetic-field induced motions of the disclination lines. Comparison of theoretical and experimental results leads to an estimate of the size of the disclination core. The elastic energy of a disclination line is obtained as a side result. A simple physical picture is given for the combined effect of the magnetic, curvature induced and dissipative forces acting on a disclination line.

1. **Introduction.** — Twisted nematic layers, sandwiched between two glass plates, have been prepared and studied ever since the beginning of this century. Mauguin [1, 2] demonstrated that such structures could be obtained by rotating one of the plates of a planar uniaxial sample through a certain angle with respect to the other. Chatelain [3] showed that such structures could also be obtained by rubbing the opposite faces of the sandwich cell in different directions prior to confining the liquid crystal between the glass plates. Recently, renewed interest in twisted nematics was aroused when the influence of electric and magnetic fields on the optical properties of a twisted nematic liquid crystal was observed [4, 5, 6, 7, 8].

In a twisted nematic prepared by rubbing the opposite surfaces in directions subtending an angle α, there are, in practice, two possible director twists in the layer [9], viz. a twist associated with a rotation of the director through an angle α, and an opposite twist corresponding to an angle of rotation $\pi - \alpha$. When $\alpha < \pi/2$, the first twist gives rise to a lower free energy density than the second one. In that case the coexistence of regions with different twist is therefore not a stable situation. For $\alpha = \pi/2$, however, a relatively stable situation can be obtained. This last case is investigated here in some detail.

The regions with opposite twist in a $\pi/2$-twisted nematic structure will be separated by a disclination line. The distortion field of the director associated with such a disclination line is calculated in section 2. When a magnetic field is applied parallel to the glass plates of the sandwich cell, the free energy densities of the regions with opposite twist will in general become different, depending on the direction of the magnetic field with respect to the mean orientation of the director in the regions. Regions with a lower free energy density will grow at the expense of regions with a higher free energy density. Consequently the bounding disclination lines will move. An expression for the velocity of the disclination line as a function of the magnetic field strength and the sample thickness is derived in section 3. The influence of the curvature of the disclination line is also considered.

In section 4 the experimental observations are reported. Line velocities are measured at different magnetic field strengths and for different sample thicknesses. Good agreement is found between theoretical and experimental results. Comparison of theoretical and experimental data enables us to give a reliable estimate of the size of the disclination core. It turns out that the combined effect of the magnetic, curvature induced and dissipative forces acting on a disclination line can be condensed into a simple physical picture. Section 5 contains some additional remarks about the experimental conditions while in

section 6 the main conclusions of the paper are summarized.

2. **Disclination line; static pattern.** — In a $\pi/2$-twisted nematic structure regions with a twist of opposite sign are separated by a disclination line. Figure 1 shows a picture of such a disclination line when viewed between parallel polarizers. The sample consists of DIBAB (p, p'-dibutylazoxybenzene) between two glass plates which have been rubbed in two mutually perpendicular directions. In the figure the rubbing directions are indicated by double-ended arrows. The directions of rubbing fix the orientation of the director at the walls. As a result of an opposite twist in the two adjacent regions, however, the director, when taken at points intermediate between the two walls, has different orientations in the two regions. When going from plate to plate it describes a certain pair of opposite right angles, which is different for each of both regions. Note that the director, on account of its non-polarity, always describes two opposite angles at the same time. The pairs of opposite right angles for the two regions are indicated by arcs in the figure. Twists of opposite sign can be made visible by optical techniques and, in the case of a negative anisotropy of the dielectric constant, also by the orientation of Williams domains (see ref. [10]).

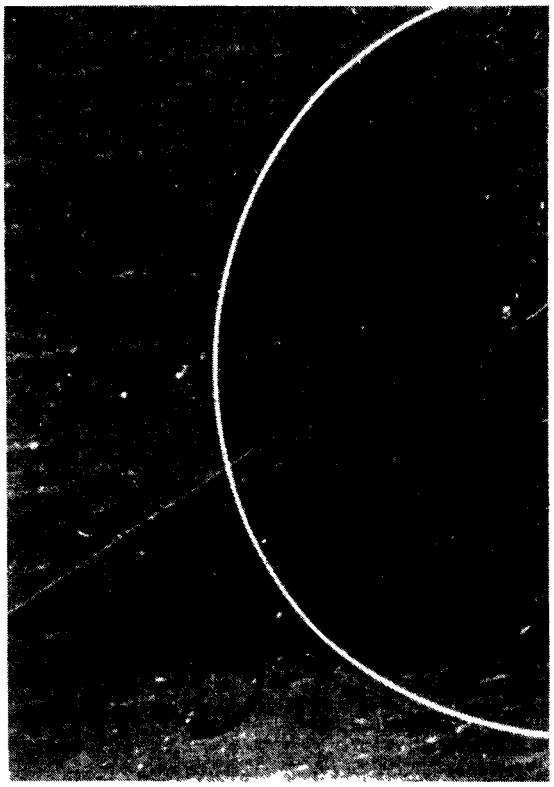

FIG. 1. — *Free* disclination line separating two regions with opposite twist in a $\pi/2$-twisted sample of DIBAB when viewed between parallel polarizers. The rubbing direction of the supporting glass plates are indicated by double-ended arrows with the arcs representing the twist angles in the two adjacent regions.

Making some weak assumptions one can calculate the distortion pattern of the director field in the neighbourhood of the disclination line. When the disclination line has a radius of curvature which is large compared with the distance $d = 2h$ of the plates, it may be considered, in a first order of approximation, as a straight line. For symmetry reasons this straight line will be situated at an equal distance h from both plates. Let us now introduce a cartesian coordinate system in which the xy-plane coincides with the plane situated midway between the two walls and the y-axis coincides with the disclination line (Fig. 2). When the director is everywhere parallel to the walls, we have

$$\mathbf{d} = \cos\varphi\mathbf{i} + \sin\varphi\mathbf{j}, \tag{2.1}$$

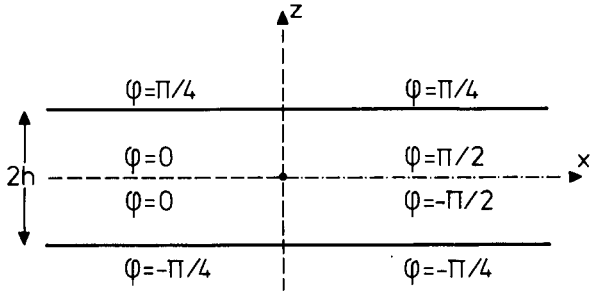

FIG. 2. — Boundary values for the director angle φ in a cross section of the $\pi/2$-twisted layer perpendicular to the disclination line (the disclination line coincides with the y-axis).

where φ denotes the angle the director subtends with the x-axis. According to our assumptions φ will be independent of y, the coordinate along the disclination line, i.e.,

$$\varphi = \varphi(x, z). \tag{2.2}$$

The director-dependent part of the free energy density is given by

$$F = \frac{1}{2}(k_{11}\sin^2\varphi + k_{33}\cos^2\varphi)\left(\frac{\partial\varphi}{\partial x}\right)^2 + \frac{1}{2}k_{22}\left(\frac{\partial\varphi}{\partial z}\right)^2. \tag{2.3}$$

Here k_{11}, k_{22} and k_{33} denote the well-known Frank constants, respectively, for splay, twist and bend. Let us assume now that

$$k_{11} = k_{33} = K. \tag{2.4}$$

Then

$$F = \frac{1}{2}K\left\{\left(\frac{\partial\varphi}{\partial x}\right)^2 + \alpha^2\left(\frac{\partial\varphi}{\partial z}\right)^2\right\}, \tag{2.5}$$

where

$$\alpha = \sqrt{\frac{k_{22}}{K}}. \tag{2.6}$$

Minimizing the total free energy for a prescribed

orientation of the director at the boundary, one obtains

$$\left(\frac{\partial^2}{\partial x^2} + \alpha^2 \frac{\partial^2}{\partial z^2}\right) \varphi = 0 . \qquad (2.7)$$

Addition of an arbitrary constant to φ leaves (2.7) clearly invariant. It is therefore possible to choose the additional constant in such a way that the boundary conditions at the walls assume the form

$$\varphi = -\frac{\pi}{4} \quad \text{at} \quad z = -h , \qquad \varphi = \frac{\pi}{4} \quad \text{at} \quad z = h . \qquad (2.8)$$

Physically speaking this means that the orientation of the disclination line with respect to the rubbing directions of the glass plates does not affect the distortion field of the director in the neighbourhood of the disclination. This property is clearly based on the assumption (2.4) that $k_{11} = k_{33}$.

Finally we should take account of the fact that the disclination line separates two regions with opposite twist. This may be done in various ways. One possibility is to consider the orientation of the director in the xy-plane. Let us assume that the left-hand region has a positive twist and accordingly the right-hand region a negative one. Then

$$\varphi = 0 \quad \text{at} \quad z = 0 , \quad \text{when} \quad x < 0 \qquad (2.9)$$

but

$$\varphi = \pm \frac{\pi}{2} \quad \text{at} \quad z = 0 , \quad \text{when} \quad x > 0 .$$

Note that the director itself experiences no discontinuity at the xy-plane. It therefore suffices to consider the upper half of the region $-h < z < h$, i.e., $0 < z < h$, for which the boundary conditions read :

$$\varphi = 0 \quad \text{at} \quad z = 0 , \quad \text{when} \quad x < 0$$

$$\varphi = \frac{\pi}{2} \quad \text{at} \quad z = 0 , \quad \text{when} \quad x > 0 \qquad (2.10)$$

$$\text{and} \quad \varphi = \frac{\pi}{4} \quad \text{at} \quad z = h .$$

The solution for the lower half can be obtained by reflection and plane symmetry.

The boundary-value problem (2.10) for the partial differential eq. (2.7) can be solved analytically. For details we refer to appendix A. The solution is given by

$$\varphi = \frac{\pi}{4} + \frac{1}{2} \arctan\left(\cot \frac{\pi z}{2h} \tanh \frac{\alpha \pi x}{2h}\right), \quad \text{when} \quad z > 0 \qquad (2.11)$$

and

$$\varphi = -\frac{\pi}{4} + \frac{1}{2} \arctan\left(\cot \frac{\pi z}{2h} \tanh \frac{\alpha \pi x}{2h}\right), \quad \text{when} \quad z < 0 .$$

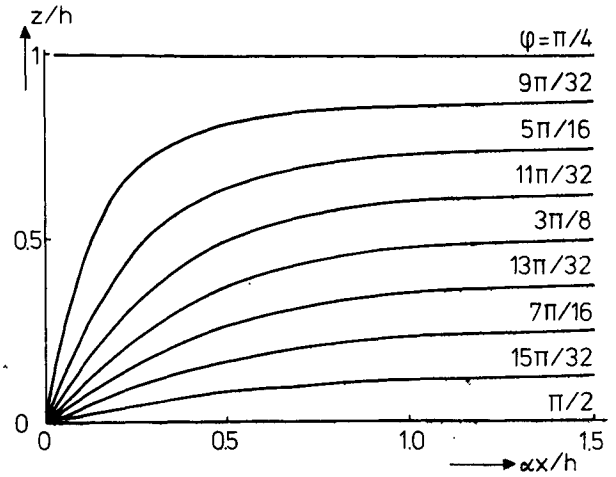

FIG. 3. — Curves φ = constant in the first quadrant of the xz-plane for a straight disclination line along the y-axis.

Figure 3 shows some curves φ = constant for the first quadrant of the xz-plane. The similar curves for the other quadrants have been omitted. The figure gives some insight into the lateral spread of the distortion field. The width of the distortion region appears to be approximately equal to the thickness of the sample.

3. **Disclination line; motions induced by a magnetic field and by curvature.** — When a magnetic field **H** is applied, the free energy density F of the nematic liquid crystal as given by (2.3) has to be supplemented by the additional magnetic energy density

$$-\frac{\chi_a}{2} (\mathbf{H}.\mathbf{d})^2 . \qquad (3.1)$$

Here $\chi_a = \chi_{//} - \chi_\perp$ denotes the (positive) anisotropy of the magnetic susceptibility of the liquid crystal. When the magnetic field is directed parallel to the walls, the additional term (3.1) simplifies to

$$-\frac{\chi_a}{2} H_0^2 \cos^2 (\varphi - \varphi_0) , \qquad (3.2)$$

where H_0 is the strength of the magnetic field and φ_0 denotes the angle it subtends with the positive x-axis. The magnetic field strength is assumed to be so low that the existing director field is not appreciably affected. This will be the case when the mean magnetic energy density (3.2) is small compared with the mean elastic energy density for the director, i.e., when

$$hH_0 \ll \frac{\alpha \pi}{2} \sqrt{\frac{K}{2\chi_a}} . \qquad (3.3)$$

Since the mean orientation of the director is different for the two regions of opposite twist (see Fig. 1), the magnetic energy densities, in general, will be different too. The disclination line will therefore tend to move in such a direction that the region of lower free energy density grows at the expense of the region

of higher free energy density. In that case the total free energy of the sample decreases. This phenomenon is observed experimentally (see section 4). During the motion of the line no flow effects are observed optically. This is not surprising since the mean rotation velocity of the director is very low ($\sim$ 0.2 rad/s.) even at the maximum magnetic field strength applied.

One also observes that the disclination line assumes a constant velocity nearly instantaneously at the moment of application of the magnetic field. This means that inertial effects may be neglected and dissipative effects are predominant. Neglecting backflow effects, we can now calculate the velocity of the disclination line by equating the loss in free energy with the energy dissipated during motion.

When u denotes the constant velocity of the disclination in the direction of the positive x-axis, the loss in free energy, taken per unit time and per unit length of the disclination line, is given by

$$u \frac{\chi_a}{2} H_0^2 \left\{ \int_{-h}^{h} \cos^2\left(\frac{\pi z}{4h} - \varphi_0\right) \mathrm{d}z - \int_{-h}^{h} \cos^2\left(\frac{\pi}{2} - \frac{\pi z}{4h} - \varphi_0\right) \mathrm{d}z \right\} = u \chi_a H_0^2 \frac{2h}{\pi} \cos 2\varphi_0 . \tag{3.4}$$

The energy dissipated during motion is caused by the local rotation of the director when the disclination line passes by. It can be shown that, in the underlying configuration, no material motions are induced by this local rotation of the director. Accordingly, the viscous couple opposing this local rotation is determined by

$$\mathbf{\Gamma}_{\text{visc}} = - \gamma_1 \frac{\partial \varphi}{\partial t} \mathbf{k} . \tag{3.5}$$

Since $\frac{\partial \varphi}{\partial t} = - u \frac{\partial \varphi}{\partial x}$, the energy dissipated per unit time and per unit length of the disclination is given by

$$\gamma_1 u^2 \int_D \int \left(\frac{\partial \varphi}{\partial x}\right)^2 \mathrm{d}x \, \mathrm{d}z . \tag{3.6}$$

Here D denotes the region of the xz-plane in which dissipation occurs. Equating (3.4) to (3.6) and using the abbreviation

$$J = \frac{1}{\alpha} \iint_D \left(\frac{\partial \varphi}{\partial x}\right)^2 \mathrm{d}x \, \mathrm{d}z \tag{3.7}$$

we obtain

$$u = \frac{\chi_a}{\alpha \gamma_1} h H_0^2 \cos(2\varphi_0) \frac{2}{\pi J} . \tag{3.8}$$

The calculation of the dissipation integral J requires closer examination. At the centre line of the disclination the orientation of the director is undetermined. When viewed on a microscopic scale, there will therefore be no long-range order of the long axes of the liquid-crystal molecules in the vicinity of the disclination centre. This means that macroscopic dissipative effects connected with this long-range order, such as dissipation resulting from rotation of the director, cannot exist in this region. But it does not necessary imply that the core is isotropic. A small cylindrical region surrounding the centre line of the disclination should therefore be excluded from the domain of integration D. The necessity of the artificial distinction between a dissipative region and a non-dissipative core is reflected by the fact that the dissipation integral J diverges logarithmically when the domain of integration D is extended to the entire neigbourhood of the disclination centre. The value of the dissipation integral J becomes consequently dependent on the size and shape of the non-dissipative core of the disclination. A plausible assumption seems to be that the disclination core has approximately a circularly cylindrical shape. Figure 3 shows that, when the diameter of the core is very small compared with the thickness $d = 2h$ of the sample and $\alpha = 1$, the circular shape can be approximated, to a very high degree of accuracy, by an orthogonal trajectory of the lines φ = constant in the vicinity of the disclination centre. This last observation facilitates the calculation of J. Details are given in appendix B. The result obtained there reads

$$J = \frac{1}{4} \left\{ \frac{\pi}{2} (1 - \log(4\kappa)) + \int_0^{\kappa} K(k) \, \mathrm{d}k - \frac{E(\kappa) - (1 - \kappa^2) K(\kappa)}{\kappa} \right. \tag{3.9}$$

where $\kappa = \sin^2 \frac{\pi b}{2h}$. Here b denotes half the diameter of the non-dissipative disclination core measured perpendicularly to the walls. The functions $K(\kappa)$ and $E(\kappa)$ are complete elliptic integrals of the first and second kind, both considered as functions of the modulus. For small values of b/h the value of J can be approximated by

$$J = \frac{\pi}{4} \left[- \log\left(\frac{\pi b}{h}\right) + \frac{1}{2} + \frac{5}{48} \left(\frac{\pi b}{h}\right)^2 \right] + + O\left(\left(\frac{\pi b}{h}\right)^4\right) . \tag{3.10}$$

This formula shows clearly the logarithmic divergence of the dissipation integral in the case where the core diameter approaches zero.

According to (3.9) the dissipation integral J is a dimensionless function of the dimensionless ratio b/h. With the aid of (3.9) numerical values can be obtained for this function. These numerical results will be presented and discussed in section 4 in connection with the experimental data.

Up to this point we have disregarded the curvature of the disclination line and accordingly assumed that the disclination line is a straight line separating two semi-infinite regions in the xy-plane. In practice, however, the disclination line, when looked upon in a direction perpendicular to the glass plates, will bound a finite region in the xy-plane. Since a finite elastic director energy is associated with each finite portion of the disclination, the disclination is able, in the absence of a magnetic field, to lower the free energy by shortening its length. The corresponding motion is observed experimentally (see section 5). The ultimate result is that the disclination line shrinks to a point and disappears, provided its motion is not hampered by *imperfections* in the sample (see Fig. 4).

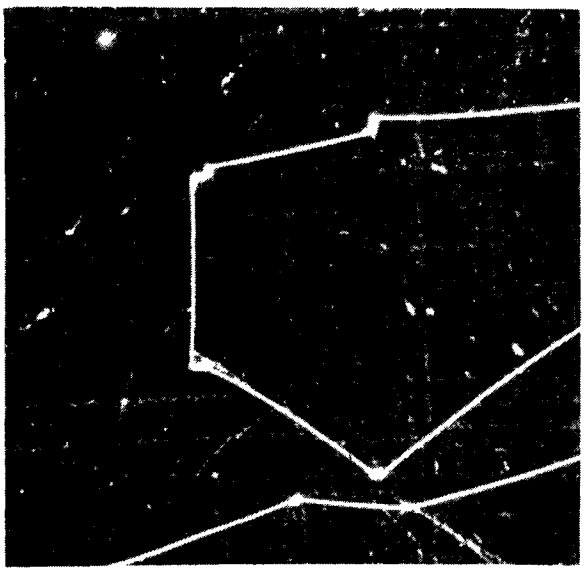

FIG. 4. — *Hampered* disclination lines in a $\pi/2$-twisted nematic layer of DIBAB when viewed between parallel polarizers.

When the disclination is a straight line coinciding with the y-axis, its elastic director energy can be calculated. Let us consider the region D_L defined by $-L < x < L$, $-h < z < h$, from which the small disclination core is excluded. It is assumed that L is large compared with the distance $2h$ between the walls. The additional free energy $\alpha KI(L)$, that results from the presence of the disclination in this region, is given by

$$\alpha KI(L) = \frac{1}{2} K \iint_{D_L} \left\{ \left(\frac{\partial \varphi}{\partial x}\right)^2 + \alpha^2 \left(\frac{\partial \varphi}{\partial z}\right)^2 \right\} dx\, dz - \frac{1}{2} \alpha^2 K \left(\frac{\pi}{4h}\right)^2 4hL . \quad (3.11)$$

Note that the last term at the right-hand side of (3.11) equals the elastic director energy in the absence of the disclination. The elastic director energy αKI associated with a unit length of the disclination can now be defined by [1]

$$\alpha KI = \alpha K \lim_{L \to \infty} I(L) . \quad (3.12)$$

An analytic expression can be obtained for I. The calculation in appendix B yields

$$I = -\frac{\pi}{8} \log (4\kappa) , \quad (3.13)$$

where $\kappa = \sin^2 \frac{\pi b}{2h}$. For a core diameter that is small compared with the sample thickness one derives from (3.13)

$$I = \frac{\pi}{4} \left[-\log \left(\frac{\pi b}{h}\right) + \frac{1}{24} \left(\frac{\pi b}{h}\right)^2 \right] + + O\left(\left(\frac{\pi b}{h}\right)^4\right) . \quad (3.14)$$

In the same way as a surface tension is associated with a surface density of the free energy, a longitudinal line tension λ is connected with the line density αKI of the disclination energy according to

$$\lambda = \alpha KI + E_{\text{core}} . \quad (3.15)$$

It is assumed that the core energy is negligible. When the disclination line is curved, this line tension gives rise to a normal force π_{el} acting on the disclination line. This force is directed towards the local centre of curvature and is given by

$$\pi_{\text{el}} = \frac{\lambda}{R} , \quad (3.16)$$

where R denotes the local radius of curvature of the disclination line. In the absence of a magnetic field this normal force must be balanced by a frictional force according to (3.6). The line density π_{diss} of this frictional force is given by

$$\pi_{\text{diss}} = -\gamma_1 \alpha J u . \quad (3.17)$$

Introducing the abbreviation

$$\hat{\eta} = \gamma_1 \alpha J , \quad (3.18)$$

we derive from (3.16) and (3.17) that, in the absence of a magnetic field,

$$\hat{\eta} u = \frac{\lambda}{R} . \quad (3.19)$$

Here u denotes the normal velocity of the disclination. In section 4 the consequences of eq. (3.19) will be

[1] Scheffer [11] calculates the elastic director energy for a twist disclination in cholesteric liquid crystals. However, he does not subtract the original twist energy in the absence of a disclination. His expression therefore becomes dependent on the outer size of the region for which the elastic director energy is calculated.

investigated with respect to the curvature-induced motions of disclination lines.

The effect of a magnetic field, too, may be interpreted as a normal force π_{magn} acting on the disclination line. This force is analogous to the Maxwell stress experienced by a deformable medium in an electromagnetic field. From (3.4) we obtain

$$\pi_{magn} = \chi_a H_0^2 \frac{2h}{\pi} \cos 2\varphi_0 . \qquad (3.20)$$

Here φ_0 denotes the angle between the magnetic field and the mean orientation of the director in that region from which the normal force is acting on the disclination. When magnetic field and curvature both influence the motion of a disclination line eq. (3.19) should be extended to

$$\hat{\eta} u = \pm \frac{\lambda}{R} + \pi_{magn} . \qquad (3.21)$$

The positive sign must be taken when the local centre of curvature lies in that region towards which the magnetic force π_{magn} and the normal line velocity u are reckoned positive. In the opposite case the minus sign must be taken. Consequences of (3.21) with respect to the shape of disclination lines that are steadily hampered by *imperfections* during their motion in a magnetic field, will be investigated in a separate paper [12].

4. **Experimental results.** — Cells containing a $\pi/2$-twisted nematic layer were prepared by sandwiching a nematic liquid crystal between two glass plates rubbed in mutually perpendicular directions. The thickness of the cells was controlled by applying various spacers with thicknesses ranging from 10 to 80 μm. The actual thickness of the empty cell was determined by optical interferometry. In order to obtain a continuous variation of thickness in one and the same sample a wedge-shaped cell was also prepared. Two liquid-crystalline compounds were used, viz, DIBAB (*p*-*p*'-dibutylazoxybenzene) and MBBA (*p*-methoxybenzilidene-*p*'-butylaniline).

A special rubbing technique was applied for providing the glass surfaces with a uniform preferred orientation. First the glass surfaces were coated with an indium oxide layer. Subsequently they were dipped into a diluted solution of an appropriate surfactant, were rubbed in the desired direction and were finally dipped again in the surfactant solution. The liquid crystal was confined between the rubbed glass plates in its isotropic-liquid phase. By cooling down into the liquid-crystalline mesophase samples were produced that showed a uniform director orientation at each of the cell walls and contained nearly exclusively freely movable disclinations (for other disclinations see ref. [13]). A typical example of such a freely movable disclination is seen in the picture of figure 1. Figure 4 shows disclination lines that are hampered by *imperfections*.

In order to move the disclination lines a magnetic field was applied parallel to the cell walls, i.e., perpendicular to the helix axis of the twisted nematic layer. The magnetic field strength chosen was of the order of 1 kOe. Therefore the condition of section 3 that the magnetic field should not affect the existing director pattern appreciably was fulfilled. The director of the magnetic field favouring the mean orientation of the director at one side of the disclination line by making an angle smaller than $\pi/4$ with this mean orientation, the disclination line was seen to move with constant velocity in such a way that the region with favoured orientation was extended.

According to (3.8) the normal velocity u is given by

$$u = \frac{\chi_a H_0^2 d}{\pi \alpha \gamma_1 J} \cos 2\varphi_0 . \qquad (4.1)$$

In order to verify this formula the velocity u was measured as a function of the magnetic field H_0 and the cell thickness $d = 2h$, the magnetic field being parallel to the mean orientation of the director at one side of the disclination line, i.e., $\varphi_0 = 0$ or $\varphi_0 = \pi/2$. The dependence on the direction of the magnetic field through $\cos 2\varphi_0$ was verified independently. The velocity u was determined by measuring the time required to move the disclination line across a well-defined distance. For that purpose a calibrated microscope was used.

First experiments were done on three cells containing DIBAB and having a thickness of 20.9, 55.4 and 78.1 μ respectively. In figure 5 the measured velocities

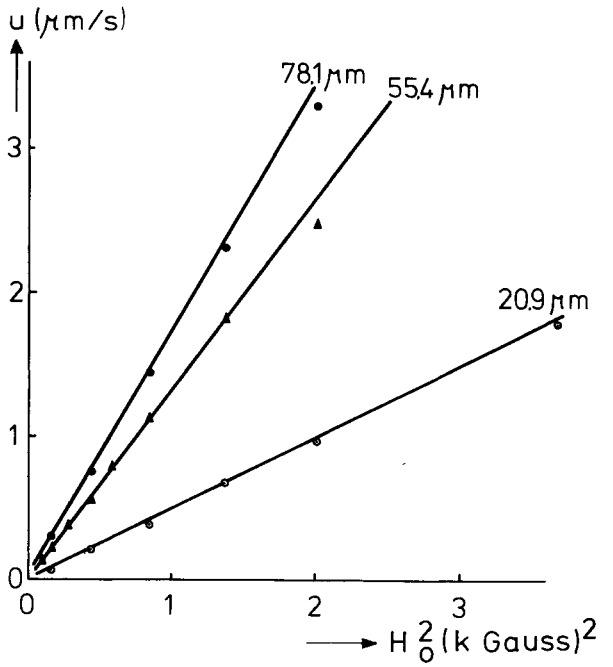

FIG. 5. — Velocity u of the disclination line measured as a function of the magnetic field strength H_0 at different thicknesses of the nematic layer.

are plotted as a function of H_0^2. It is seen that the relation between u and H_0^2 is perfectly linear provided the magnetic field strength is not too high. The second column of table I gives the numerical values of the slopes u/H_0^2 of the three lines of figure 5. In the third column the values of $u/H_0^2\,d$ are presented. Since $u/H_0^2\,d$ has nearly the same value for the three samples, one is inclined to conclude that u depends linearly on d. In addition it follows that $J(b/h)$ cannot depend on h, i.e., that the core diameter $2\,b$ of the disclination is *proportional* to the thickness $d = 2\,h$ of the nematic layer. We shall return to this point later on in this section.

TABLE I

Measured values of u/H_0^2 *and* $u/H_0^2\,d$ *at different thicknesses* d *for samples containing* DIBAB

d [μm]	u/H_0^2 [cm(kOe)$^{-2}$ s^{-1}]	$u/H_0^2\,d$ [(kOe)$^{-2}$ s^{-1}]
—	—	—
20.9	0.49	0.023
55.4	1.33	0.024
78.1	1.70	0.022

To investigate the dependence of u on d a wedge-shaped cell was taken, for which the thickness d is a linear function of the distance x from the cell edge. The liquid-crystalline material was again DIBAB. Figure 6 shows the disclination velocity u as a function of the distance x along the cell in the case that

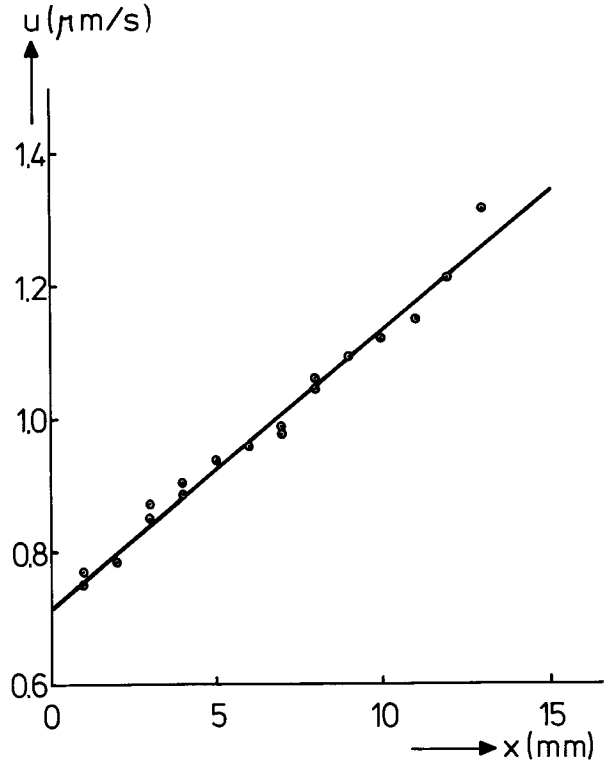

FIG. 6. — Velocity u of the disclination line in a wedge-shaped sample measured as a function of cell thickness at a constant magnetic field of 1.1 kG.

$H_0 = 1.1$ kOe and $\varphi_0 = 0$. The experimental results show indeed a perfect linear dependence.

The optical boundary of the line is defined as the edge, where the light intensity starts to differ significantly from its minimum value, when viewed under a microscope between two parallel or perpendicularly oriented polarizers. Measurements of the optical width yield the following results.

— The width is *independant* of cell thickness.

— The width depends on the mutual orientation of the polarizers.

— Between crossed and parallel polarizers the values for the width are 0.6 μm and 2.5 μm respectively.

This may be explained as follows. According to Mauguin [1] the transmission of plane polarized light through a twisted nematic layer is determined by a quantity $f = 2\,\lambda/p.\,\Delta n$, where λ is the wavelength of light, Δn is the optical anisotropy of the liquid crystal and $p = 2\,\pi(\mathrm{d}z/\mathrm{d}\varphi)$ is the local pitch. When $f < 1$ the light remains nearly plane polarized and the polarisation direction *follows* the twist in the case of normally incident light. When $f > 1$ the incident light does not *follow* the twist anymore. The value of $\mathrm{d}z/\mathrm{d}\varphi$ can be calculated from eq. (2.11). It attains its minimum value for a constant value of x at $z = 0$. At $z = 0$ and small values of x, $\mathrm{d}z/\mathrm{d}\varphi$ can be approximated by $2\,\alpha x$. If $x = \frac{1}{2}\,w$, where w is the optical width of the disclination line the values of f at the observed edges of the disclination are 0,5 and 2.0 in the case of parallel and perpendicular polarizers respectively. Clearly $\mathrm{d}z/\mathrm{d}\varphi$ is independent of cell thickness. We therefore conclude that the optical width of the $S = \frac{1}{2}$ disclination in a twisted nematic is not directly related to the core diameter, but does depend on the director pattern in the neighbourhood of the line.

Since the core diameter calculated from the dynamic properties of the disclination is of the same magnitude as the optical width, an isotropic core is not the right model for the core. Only the reduction of the long-range order within the calculated core seems a more likely model.

It was agreed already that J should have a constant value independent of the thickness d of the cell. When the material constants χ_a, α and γ_1 are known, it is possible to determine this value of J from the measured velocities by means of (4.1). Unfortunately the material constants are not known for DIBAB at this time. Therefore some experiments were performed with twisted layers of pure MBBA ($T_c = 47.5$ °C) for which substance α, γ_1 and χ_a are known as a function of temperature.

The mean value obtained for $u/H_0^2\,d$ at 22 °C is 0.018 (kOe)$^{-2}$ s^{-1}. Substituting this mean value in (4.1) and using the known values $\chi_a = 0.93 \times 10^{-7}$ [14], $\gamma_1 = 1.25$ [14, 15] and $k_{11}/k_{22} = 2.0$ [16] in cgs units for MBBA we finally obtain for J the value listed in the second column of table II.

TABLE II

Experimental values for the dissipation integral J, the ratio of the core diameter to the layer thickness b/h and the elastic director energy I obtained on samples containing MBBA.

J	$2/\pi J$	b/h	$2/\pi I$	I
1.9	0.34	4.8×10^{-2}	0.42	1.5

Under a reasonable assumption for the shape of the disclination core we have derived the exact formula (3.9) for the dissipation integral J as a function of b/h, the ratio of the core diameter to the layer thickness. By means of this formula numerical values have been obtained for $2/\pi J$ at different values of b/h. They are plotted as a solid curve in figure 7. The corresponding dashed curve shows the values that are obtained when the approximation formula

$$J = \frac{\pi}{4}\left[-\log\left(\frac{\pi b}{h}\right) + \frac{1}{2}\right] \qquad (4.2)$$

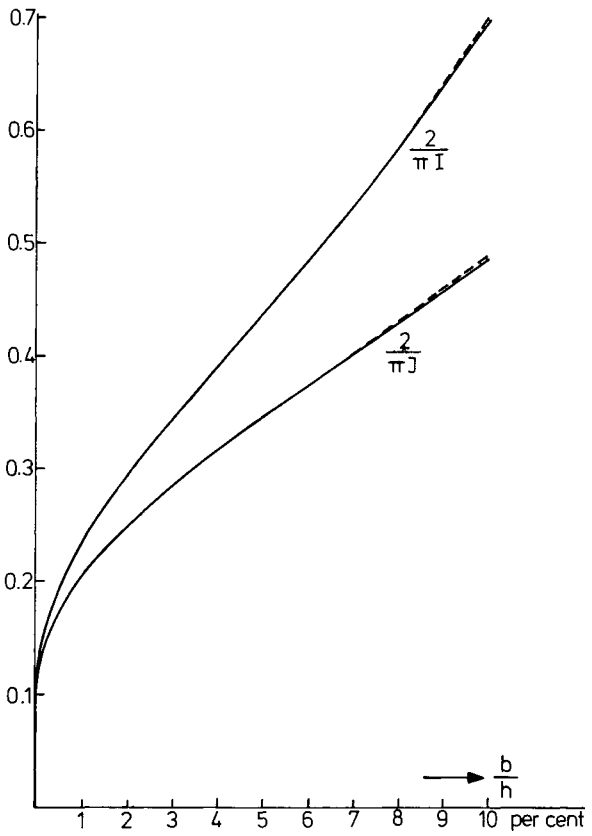

FIG. 7. — The reciprocal dissipation integral $2/\pi J$ and the reciprocal elastic energy integral $2/\pi I$ plotted as a function of b/h ($2\,b$ = core diameter, $2\,h$ = cell thickness) according to eqs. (3.9) and (3.13).

is used (cf. (3.10)). It can be shown that this last formula for J does not depend on the assumed shape of the disclination core. It turns out that the approximation formula can be used at values of b/h as large as 8×10^{-2}. From the experimental value for J it is now possible to determine the corresponding value of b/h by means of the curve for $2/\pi J$ in figure 7. The resulting value is presented in the third column of table II. It lies within the region where the approximation formula (4.2) can be used safely. It should be noted that the value derived for b/h only gives an estimate of the size of the disclination core. This is connected with the fact that relative changes of the magnitude of the dissipation integral J are not very sensitive to relative changes of the value of b/h. This last observation is consistent with the more or less artificial introduction of the non-dissipative disclination core as an auxiliary quantity into the calculations.

Formula (3.13) gives the value of I, the integral for the elastic director energy, as a function of b/h. The second solid curve in figure 7 shows the numerical values obtained for $2/\pi I$ by means of this formula. The corresponding dashed curve presents the results in the case when the approximation formula

$$I = \frac{\pi}{4}\left[-\log\left(\frac{\pi b}{h}\right)\right] \qquad (4.3)$$

is used (cf. (3.14)). Note that in the region where both approximation formulas (4.2) and (4.3) are valid

$$I\left(\frac{b}{h}\right) = J\left(\frac{b}{h}\right) - \frac{\pi}{8} \approx J\left(\frac{b}{h}\right) - 0.39\,. \qquad (4.4)$$

Assuming now that the diameter of the disclination core is the same for the elastic effects contained in I as for the dissipative effects accounted for by J we are able to derive by means of (4.4) an experimental value for the elastic director energy I. It is found in the last column of table II.

5. **Additional remarks.** — Sometimes the disclination lines are seen to move in the absence of a magnetic field. This motion may be partially attributed to the fact that the rubbing directions of the bounding glass surfaces of the cell are not exactly perpendicular. In that case the twist-energy densities at opposite sides of the disclination line are not exactly equal and a slow motion of the disclination line results favouring the region of smaller twist-energy density.

Also curvature induced motions are observed in the absence of a magnetic field. When the core energy is negligible with respect to the elastic energy these motions are according to (3.19), (3.17) determined by

$$u = \frac{I}{J}\,\frac{K}{\gamma_1}\,\frac{1}{R}\,, \qquad (5.1)$$

R being the local radius of curvature of the disclination line. In the case of MBBA, $K = k_{33} = 0.85 \times 10^{-6}$ dyn [16] $\gamma_1 = 1.25$ dyn cm^{-2} s [15], while according to table II $I/J = 0.79$. It follows that for MBBA

$$u = 0.54 \times 10^{-6}\,\frac{1}{R} \qquad (5.2)$$

in cgs units. This means that a circular disclination line having a radius of 100 μm shrinks with a radial velocity of about 0.5 μm/s. The validity of (5.2) has been investigated experimentally, with the result that $u = 1.5 \times 10^{-6} \frac{1}{R}$. The assumption of a small core energy seems therefore justified. For details we refer to [17].

The zero-field velocities discussed in the preceding two paragraphs have been corrected for during the experiments by reversing the direction of motion, i.e., by determining the line velocities at $\varphi_0 = 0$ and $\varphi_0 = \pi/2$, and taking the average of the absolute value of the velocity measured in both cases.

When a moving disclination line contacts a dust particle present in the sample, this dust particle usually adheres to the line. At the point of contact with the particle the line stops. In the neighbourhood of the point of contact the disclination line gets curved. At the same time the particle is accelerated. This accelerating force can be attributed to the line tension of the disclination which shows a discontinuous tangent at the point of contact. After some time a steady situation is arrived at, in which the curved line and the adhering dust particle move at constant speed. The theoretical shape of such a disclination line with an adhering particle can be derived from (3.21). For theoretical and experimental results we refer to [13].

The velocity change caused by an adhering dust particle cannot be corrected for by reversing the direction of motion of the disclination line. However, the chance of particles being picked up by the moving line can be reduced considerably by applying a low electric voltage across sample electrodes for several minutes. Another method consists of cleaning parts of the cell by means of a moving disclination line. The line is first moved slowly in one direction so that it carries with it all particles encountered and next moved at high speed in the reverse direction. During this high speed motion the particles are detached from the disclination line. Apparently the line tension is too small to balance the relatively large viscous drag experienced by the particles during this high-speed motion.

6. **Conclusions.** — Disclination lines separating regions of opposite twist in twisted nematic structures can be moved by applying a magnetic field perpendicular to the twist axis. The local velocity of the disclination line turns out to be proportional to the square of the magnetic field strength and to the sample thickness. Theoretical arguments show that the constant of proportionality depends, besides on some material constants of the nematic liquid crystal, on a dimensionless quantity J, here called the dissipation integral. According to theory this dissipation integral J is a well-defined function of b/h, the ratio of the diameter of the disclination core to the sample thickness. From measured values of the line velocities it is derived that

$$J \approx 1.9 .$$

The diameter $2b$ of the disclination core is roughly proportional to the sample thickness $2h$, their ratio b/h lying between 4 and 5 per cent. This is contrary to the model of a core having molecular dimensions [18].

As a side result the elastic director energy of a disclination line is obtained. When the dissipative domain D of eq. (3.6) coincides with the elastic domain D_L (3.11) the dimensionless integral I entering the energy is given by eq. (4.4) with the result that

$$I \approx 1.5 .$$

For an experimental verification of this derived value for I we refer to [17].

Due to the fact that the shrinkage of disclination loops could be explained for a large part by the elastic energy of the director pattern, the core is not supposed to be in an isotropic state. The measured line energy does not exceed the elastic energy strongly. Also not any optical influence on the line width was observed as should be expected from the assumption of an isotropic core.

APPENDIX A

In section 2 the following boundary-value problem was formulated. Find the function $\varphi(x, z)$ that satisfies within the strip $-\infty < x < \infty$, $0 < z < h$, the partial differential equation

$$\left(\frac{\partial^2}{\partial x^2} + \alpha^2 \frac{\partial^2}{\partial z^2}\right) \varphi = 0 , \tag{2.7}$$

and assumes the boundary values

$$\begin{aligned} &\varphi = 0 \quad \text{at} \quad z = 0 \quad \text{when} \quad x < 0 \\ &\varphi = \frac{\pi}{2} \quad \text{at} \quad z = 0 \quad \text{when} \quad x > 0 \\ &\varphi = \frac{\pi}{4} \quad \text{at} \quad z = h . \end{aligned} \tag{2.10}$$

The coordinate transformation

$$\tilde{x} = \alpha x , \quad \tilde{z} = z \tag{A.1}$$

reduces the partial differential eq. (2.7) to Laplace's equation

$$\left(\frac{\partial^2}{\partial \tilde{x}^2} + \frac{\partial^2}{\partial \tilde{z}^2}\right) \varphi = 0 , \tag{A.2}$$

while the boundary conditions (2.10) retain their original form. The boundary-value problem for the harmonic function $\varphi = \tilde{\varphi}(\tilde{x}, \tilde{z})$ may be solved in various ways. With a view to the calculations in

appendix B we shall use here the technique of conformal mapping.

The harmonic function $\varphi = \tilde{\varphi}(\tilde{x}, \tilde{z})$ can be considered as the imaginary part of a complex function $\Phi = \chi + i\varphi$ that is holomorphic when considered as a function of the complex variable $Z = \tilde{x} + i\tilde{z}$ in the strip $0 < \text{Im}\, Z < h$. Note that χ is a harmonic function $\chi = \tilde{\chi}(\tilde{x}, \tilde{z})$ conjugate to the harmonic function $-\tilde{\varphi}(\tilde{x}, \tilde{z})$. Because of reflection symmetry

$$\Phi(Z^*) = \Phi^*(Z), \qquad (A.3)$$

where an asterisk denotes the complex conjugate value. For the holomorphic function $\Phi(Z)$ we have the following boundary-value problem (see Fig. 8)

$$\begin{aligned} &\text{Im}\, \Phi = 0 \text{ when } \text{Im}\, Z = 0, \ -\infty < \text{Re}\, Z < 0, \\ &\text{Im}\, \Phi = \frac{\pi}{2} \text{ when } \text{Im}\, Z = 0, \quad 0 < \text{Re}\, Z < \infty, \\ &\text{Im}\, \Phi = \frac{\pi}{4} \text{ when } \text{Im}\, Z = h, \ -\infty < \text{Re}\, Z < \infty. \end{aligned} \qquad (A.4)$$

The transformation

$$\zeta = e^{\pi Z/h}, \qquad Z = \frac{h}{\pi} \log \zeta \qquad (A.5)$$

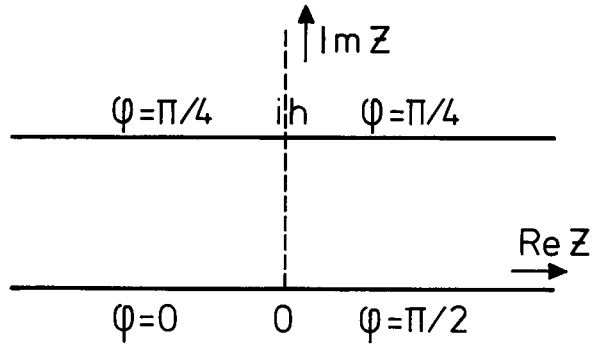

FIG. 8. — Boundary values for $\chi + i\varphi = \Phi(Z)$ in the strip $0 < \text{Im}\, Z < h$ of the complex Z-plane.

maps the strip $0 < \text{Im}\, Z < h$ of the complex Z-plane conformally onto the upper half of the complex ζ-plane. The function $\Phi(Z)$ is transformed into a function $\Psi(\zeta) = \Phi(Z(\zeta))$ that is holomorphic in the upper half of the complex ζ-plane. The corresponding boundary-value problem for $\Psi(\zeta)$ reads (see Fig. 9)

$$\begin{aligned} &\text{Im}\, \Psi = \frac{\pi}{4} \text{ when } \text{Im}\, \zeta = 0, \ -\infty < \text{Re}\, \zeta < 0, \\ &\text{Im}\, \Psi = 0 \text{ when } \text{Im}\, \zeta = 0, \quad 0 < \text{Re}\, \zeta < 1, \\ &\text{Im}\, \Psi = \frac{\pi}{2} \text{ when } \text{Im}\, \zeta = 0, \quad 1 < \text{Re}\, \zeta < \infty. \end{aligned} \qquad (A.6)$$

The solution of (A.6) can be obtained by inspection. It is given by

$$\Psi(\zeta) = \frac{1}{4} \log \zeta - \frac{1}{2} \log (\zeta - 1) + i\frac{\pi}{2} + \chi_0, \qquad (A.7)$$

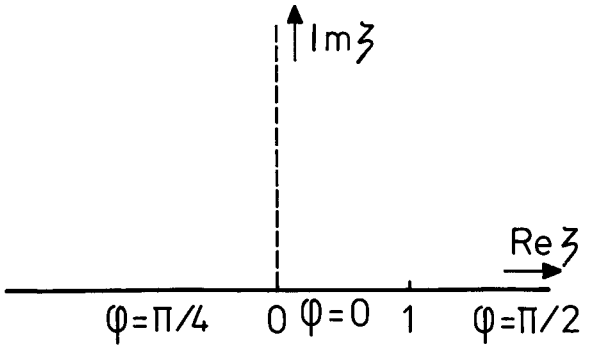

FIG. 9. — Boundary values for $\chi + i\varphi = \Psi(\zeta)$ in the upper half of the complex ζ-plane.

where χ_0 is an arbitrary real constant. We take $\chi_0 = 0$ Backward transformation yields

$$\Phi(Z) = -\frac{1}{2} \log \left(2 \sinh \frac{\pi}{2} \frac{Z}{h}\right) + i\frac{\pi}{2}. \qquad (A.8)$$

Taking real and imaginary parts we finally obtain

$$\chi = -\frac{1}{2} \log 2 - \frac{1}{4} \log \left(\sinh^2 \frac{\pi\alpha x}{2h} \cos^2 \frac{\pi z}{2h} + \cosh^2 \frac{\pi\alpha x}{2h} \sin^2 \frac{\pi z}{2h}\right), \qquad (A.9)$$

$$\varphi = \frac{\pi}{4} + \frac{1}{2} \arctan \left(\tanh \frac{\pi\alpha x}{2h} \cot \frac{\pi z}{2h}\right). \qquad (A.10)$$

Note that (A.10) is only valid when $z > 0$. When $z < 0$, we have according to the symmetry relation (A.3)

$$\varphi = -\frac{\pi}{4} + \frac{1}{2} \arctan \left(\tanh \frac{\pi\alpha x}{2h} \cot \frac{\pi z}{2h}\right). \qquad (A.11)$$

APPENDIX B

In section 3 the dissipation integral J was defined by

$$J = \frac{1}{\alpha} \iint_D \left(\frac{\partial \varphi}{\partial x}\right)^2 dx\, dz \qquad (3.7)$$

the domain of integration D being the region of the xz-plane in which dissipation occurs. By means of the coordinate transformation (A.1) the expression for J passes into

$$J = \iint_{\tilde{D}} \left(\frac{\partial \varphi}{\partial \tilde{x}}\right)^2 d\tilde{x}\, d\tilde{z}, \qquad (B.1)$$

where $\tilde{D}$ is the corresponding domain of integration in the $\tilde{x}\tilde{z}$-plane.

Since φ may be considered as the imaginary part of a holomorphic function $\Phi = \chi + i\varphi$ of $Z = \tilde{x} + i\tilde{z}$ (see appendix A), we have

$$\frac{\partial \varphi}{\partial \tilde{x}} = \text{Im}\left(\frac{d\Phi}{dZ}\right) = \frac{1}{2i}\left\{\frac{d\Phi}{dZ} - \left(\frac{d\Phi}{dZ}\right)^*\right\}. \qquad (B.2)$$

Here an asterisk denotes again the complex conjugate value. Furthermore

$$d\tilde{x}\, d\tilde{z} = \left| \frac{d\Phi}{dZ} \right|^{-2} d\chi\, d\varphi = \left\{ \frac{d\Phi}{dZ} \left(\frac{d\Phi}{dZ} \right)^* \right\}^{-1} d\chi\, d\varphi . \quad (B.3)$$

Substituting (B.2) and (B.3) into (B.1) one obtains

$$J = -\frac{1}{4} \iint_{\Delta} \left\{ 2 - \frac{d\Phi}{dZ} \Big/ \left(\frac{d\Phi}{dZ} \right)^* - \left(\frac{d\Phi}{dZ} \right)^* \Big/ \frac{d\Phi}{dZ} \right\} d\chi\, d\varphi . \quad (B.4)$$

The domain of integration Δ in the $\chi\varphi$-plane corresponds to the domain of integration $\tilde{D}$ in the $\tilde{x}\tilde{z}$-plane. In section 3 the boundary of the non-dissipative core of the disclination was assumed to be determined by an orthogonal trajectory of the lines φ = constant. This means that the boundary of the disclination core coincides with a curve characterised by a constant value of χ, say $\chi = X$. For a small core diameter X will be a large positive constant (compare (A.9)). The domain of integration Δ is therefore given by

$$-\infty < \chi < X, \qquad -\frac{\pi}{2} < \varphi < \frac{\pi}{2} . \quad (B.5)$$

According to (A.8)

$$Z = -\frac{2h}{\pi} \operatorname{arsinh} \left(\frac{1}{2} e^{-2\Phi} \right) . \quad (B.6)$$

Hence

$$\frac{dZ}{d\Phi} = \frac{4h}{\pi} (1 + 4 e^{4\Phi})^{-1/2} . \quad (B.7)$$

Substituting (B.7) into (B.4) and taking account of (B.5) we obtain

$$J = \frac{1}{4} \int_{-\infty}^{X} \int_{-\pi/2}^{\pi/2} \left\{ 2 - \left(\frac{1 + 4 e^{4\Phi}}{1 + 4 e^{4\Phi^*}} \right)^{1/2} + \left(\frac{1 + 4 e^{4\Phi^*}}{1 + 4 e^{4\Phi}} \right)^{1/2} \right\} d\chi\, d\varphi$$

$$= \frac{1}{4} \int_{-\infty}^{X} d\chi \int_{-\pi/2}^{\pi/2} d\varphi \left\{ 2 - \left[2 - \frac{(4 e^{2\chi})^2}{1 + 4 e^{4\chi}} \sin^2 2\varphi \right] \times \left[1 - \left(\frac{4 e^{2\chi}}{1 + 4 e^{4\chi}} \right)^2 \sin^2 \varphi \right]^{-1/2} \right\} . \quad (B.8)$$

Introducing the usual notation for complete elliptic integrals of the first and second kind, viz.,

$$K(k) = \int_0^{\pi/2} (1 - k^2 \sin^2 \theta)^{-1/2}\, d\theta ,$$
$$E(k) = \int_0^{\pi/2} (1 - k^2 \sin^2 \theta)^{1/2}\, d\theta , \quad (B.9)$$

one can write

$$J = \frac{1}{2} \int_{-\infty}^{X} d\chi \{ \pi - (1 - 4 e^{4\chi}) K(k) + (1 + 4 e^{4\chi}) E(k) \} , \quad (B.10)$$

where the modulus k is given by

$$k = \frac{4 e^{2\chi}}{1 + 4 e^{4\chi}} . \quad (B.11)$$

The complementary modulus k', defined by $k' = (1 - k^2)^{1/2}$ is expressed in terms of χ by

$$k' = \begin{cases} \dfrac{1 - 4 e^{4\chi}}{1 + 4 e^{4\chi}} & \text{when } \chi < -\frac{1}{2} \log 2 \\ \dfrac{1 - \frac{1}{4} e^{-4\chi}}{1 + \frac{1}{4} e^{-4\chi}} & \text{when } \chi > -\frac{1}{2} \log 2 . \end{cases} \quad (B.12)$$

With the aid of (B.12) the expression (B.10) for J may be written as

$$J = \int_{-\infty}^{-(1/2)\log 2} d\chi \left\{ \frac{\pi}{2} - \frac{E(k) + k' K(k)}{1 + k'} \right\} + \int_{-(1/2)\log 2}^{X} d\chi \left\{ \frac{\pi}{2} - \frac{E(k) - k' K(k)}{1 - k'} \right\} . \quad (B.13)$$

According to Gauss's quadratic transformation (19)

$$K(k_1) = \frac{1 + k'}{2} K(k) ,$$
$$E(k_1) = \frac{E(k) + k' K(k)}{1 + k'} , \quad (B.14)$$

where $k_1 = \dfrac{1 - k'}{1 + k'}$. Note that in the underlying case

$$k_1 = \begin{cases} 4 e^{4\chi} & \text{when } \chi < -\frac{1}{2} \log 2 \\ \frac{1}{4} e^{-4\chi} & \text{when } \chi > -\frac{1}{2} \log 2 . \end{cases} \quad (B.15)$$

Using (B.14) and (B.15) we derive from (B.13) that

$$J = \frac{1}{4} \left[\int_0^1 dk_1 \left\{ \frac{\pi}{2} - E(k_1) \right\} \Big/ k_1 + \int_{\kappa}^1 dk_1 \left\{ \frac{\pi}{2} - \frac{E(k_1) - (1 - k_1^2) K(k_1)}{k_1} \right\} \Big/ k_1 \right] . \quad (B.16)$$

Here

$$\kappa = \frac{1}{4} e^{-4\chi} . \quad (B.17)$$

It is known that [19]

$$\int_0^1 \left\{ E(k) - \frac{\pi}{2} \right\} \frac{\mathrm{d}k}{k} = \frac{1}{2}(2\pi \log 2 - 4G + 2 - \pi) \quad \text{(B.18)}$$

and

$$\int \frac{K(k) - E(k)}{k^2} \mathrm{d}k = \frac{E(k) - (1 - k^2) K(k)}{k} . \quad \text{(B.19)}$$

Here G denotes Catalan's constant given by

$$G = \frac{1}{2} \int_0^1 K(k) \, \mathrm{d}k \approx 0.915\,965\,6 . \quad \text{(B.20)}$$

We therefore finally obtain

$$J = \frac{1}{4} \left[\frac{\pi}{2} \{ 1 - \log (4\kappa) \} - \frac{E(\kappa) - (1 - \kappa^2) K(\kappa)}{\kappa} + \int_0^\kappa K(k) \, \mathrm{d}k \right] . \quad \text{(B.21)}$$

The value of κ defined by (B.17) can be calculated from

$$\kappa = \sin^2 \frac{\pi b}{2h} , \quad \text{(B.22)}$$

where b denotes half the diameter of the non-dissipative kernel measured perpendicularly to the walls.

Finally an analytic expression will be given for the elastic director energy αKI of the disclination. According to (3.11) and (3.12)

$$I = \lim_{L \to \infty} \frac{1}{2} \left[\frac{1}{\alpha} \iint_{D_L} \left\{ \left(\frac{\partial \varphi}{\partial x} \right)^2 + \alpha^2 \left(\frac{\partial \varphi}{\partial z} \right)^2 \right\} \mathrm{d}x \, \mathrm{d}z - \alpha \left(\frac{\pi}{4h} \right)^2 4hL \right] . \quad \text{(B.23)}$$

Applying the transformation (A.1) and using (B.3) we obtain

$$I = \lim_{L \to \infty} \frac{1}{2} \left[\iint_{\Delta_L} \mathrm{d}\varphi \, \mathrm{d}\chi - \alpha \left(\frac{\pi}{4h} \right)^2 4hL \right] , \quad \text{(B.24)}$$

where the domain of integration Δ_L in the $\chi\varphi$-plane corresponds to the domain of integration D_L in the xz-plane. It follows from (A.9) that for large values of L

$$\chi = - \alpha \frac{\pi L}{4h} + O(\mathrm{e}^{-\pi L/h}) . \quad \text{(B.25)}$$

We therefore derive from (B.24) that

$$I = \frac{\pi}{2} X . \quad \text{(B.26)}$$

Note that the boundary of the disclination core is assumed to be given by $\chi = X$. With the aid of (B.17) and (B.22) the expression (B.26) for I can be written as

$$I = - \frac{\pi}{8} \log (4\kappa) \quad \text{(B.27)}$$

with

$$\kappa = \sin^2 \frac{\pi b}{2h} .$$

References

[1] MAUGUIN, Ch., *Bull. Soc. Fr. Minéral.* **34** (1911) 71.
[2] MAUGUIN, Ch., *Z. Phys.* **12** (1911) 1010.
[3] CHATELAIN, P., *Bull. Soc. Fr. Minéral.* **66** (1943) 105.
[4] LESLIE, F. M., *Mol. Cryst. Liq. Cryst.* **12** (1970) 57.
[5] SCHADT, M. and HELFRICH, W., *Appl. Phys. Lett.* **18** (1971) 127.
[6] GERRITSMA, C. J., DE JEU, W. H. and VAN ZANTEN, P., *Phys. Lett.* **36A** (1971) 389.
[7] SHTRIKMAN, S., WOHLFARTH, E. P. and WAND, Y., *Phys. Lett.* **37A** (1971) 369.
[8] VAN DOORN, C. Z., *Phys. Lett.* **42A** (1973) 537.
[9] MEYER, R. B., *Colloque sur les Cristaux Liquides*, Pont-à-Mousson (France), 1971.
[10] GERRITSMA, C. J., GEURST, J. A. and SPRUIJT, A. M. J., *Phys. Lett.* **43A** (1973) 356.
[11] SCHEFFER, T. J., *Phys. Rev.* **A 5** (1972) 1327.
[12] GEURST, J. A. and SPRUIJT, A. M. J., to be published.
[13] SPRUIJT, A. M. J., *Solid State Commun.* **13** (1973) 1919.
[14] GASPAROUX, H. and PROST, J., *J. Physique* **32** (1971) 953.
[15] BROCHARD, F., PIERANSKI, P. and GUYON, E., *Phys. Rev. Lett.* **28** (1972) 1681.
[16] HALLER, I., *J. Chem. Phys.* **57** (1972) 1400.
[17] SPRUIJT, A. M. J. and GEURST, J. A., to be published, in part presented at the Fifth International Liquid Crystal Conference, Stockholm 1974.
[18] DE GENNES, P. G., *C. R. Hebd. Séan. Acad. Sci.* B **266** (1968) 571.
[19] BYRD, P. F. and FRIEDMAN, M. D., *Handbook of Elliptic Integrals for Engineers and Physicists* (Springer Verlag, Berlin) 1954.